J|A|C|S
ARTICLES

Published on Web 02/09/2009

Crystallographic Characterization of Helical Secondary Structures in 2:1 and 1:2 α/β-Peptides

Soo Hyuk Choi, Ilia A. Guzei, Lara C. Spencer, and Samuel H. Gellman*

Department of Chemistry, University of Wisconsin, Madison, Wisconsin 53706

Received October 16, 2008; E-mail: gellman@chem.wisc.edu

Abstract: Oligomers containing both α- and β-amino acid residues ("α/β-peptides") are intriguing as potential foldamers. A large set of α/β-peptide backbones can be generated by combining α- and β-amino acid residues in different patterns; however, most research to date has focused on the simplest pattern, 1:1 α:β. We have begun to explore the range of variation that can be achieved with α-residue/β-residue combinations by examining the folding behavior of oligomers that contain 2:1 and 1:2 α:β patterns. The β-residues in our systems have a five-membered-ring constraint (*trans*-2-aminocyclopentanecarboxylic acid (ACPC) residues), because these preorganized subunits strongly promote helical folding for 1:1 α:β backbones and pure β backbones. Previously we concluded that two helical conformations are available to 2:1 and 1:2 α/β-peptides containing ACPC or analogously constrained β-residues, one helix defined by *i*,*i*+3 C=O···H−N backbone hydrogen bonds and the other defined by *i*,*i*+4 C=O···H−N hydrogen bonds. These deductions were based on 2D NMR analysis of a 2:1 heptamer and a 1:2 hexamer in methanol. Crystallographic analysis of a pair of analogous nonpolar α/β-peptides showed only the *i*,*i*+3 hydrogen-bonded helical conformations. We now report four new crystal structures of 2:1 α/β-peptides, ranging in length from 5 to 11 residues, and six new crystal structures of 1:2 α/β-peptides, ranging in length from 6 to 10 residues. All 10 of these new structures are fully helical, and all helices display the *i*,*i*+3 C=O···H−N hydrogen bonding pattern. These crystallographic data sets, collectively, provide high structural definition for the *i*,*i*+3 hydrogen-bonded helical secondary structures available to these foldamer backbones.

Introduction

The diverse functions of proteins usually require adoption of specifically folded conformations, which are dictated by the α-amino acid sequence. The relationship between subunit sequence (one-dimensional information) and molecular shape (three-dimensional information) among poly-α-peptides has inspired many researchers to explore unnatural oligomers for the ability to adopt distinct conformations, that is, to behave as "foldamers".[1] Well-defined molecular shapes should provide a basis for generating useful function, and this prospect provides a long-term motivation for foldamer research. Several groups have reported oligomers with strong folding propensities that have been engineered to display interesting properties, such as a specific biological activity.[1d] These efforts have revealed that success in function-oriented design can depend critically upon access to multiple foldamer scaffolds, each of which provides a distinctive way to orient sets of side chains in space.

Recent efforts to expand the set of oligomeric backbones with established folding propensities have included the exploration of "heterogeneous" systems,[2−9] that is, oligomers that contain more than one type of building block. Biopolymer prototypes, such as proteins and nucleic acids, have homogeneous backbones: all subunits have the same set of backbone atoms and differ only in the side chains. It is tempting to speculate that the exigencies of evolving reliable mechanisms for template-directed biopolymer synthesis strongly favored backbones with an invariant backbone repeat element. Many of the first-generation foldamers that emerged in the 1990s, such as β-amino acid oligomers,[10] phenylene ethynylene oligomers,[11] and aminoxy acid oligomers,[12] have homogeneous backbones as well. However, recent efforts to expand the foldamer universe have frequently involved backbones that contain two different types of subunit, for example, combination of α-amino acid residues with α-aminoxy acid residues,[2] with β-amino acid residues,[3−7]

(1) (a) Gellman, S. H. *Acc. Chem. Res.* **1998**, *31*, 173. (b) Hill, D. J.; Mio, M. J.; Prince, R. B.; Hughes, T. S.; Moore, J. S. *Chem. Rev.* **2001**, *101*, 3893–4011. (c) Hecht, S., Huc, I., Eds. *Foldamers: Structure, Properties and Applications*; Wiley-VCH: Weinheim, Germany, 2007. (d) Goodman, C. M.; Choi, S.; Shandler, S.; DeGrado, W. F. *Nat. Chem. Biol.* **2007**, *3*, 252.

(2) Yang, D.; Li, W.; Qu, J.; Luo, S. W.; Wu, Y. D. *J. Am. Chem. Soc.* **2003**, *125*, 13018.

(3) (a) Chatterjee, S.; Roy, R. S.; Balaram, P. *J. R. Soc. Interface* **2007**, *4*, 587. (b) Horne, W. S.; Gellman, S. H. *Acc. Chem. Res.* **2008**, *41*, 1399.

(4) (a) Hayen, A.; Schmitt, M. A.; Ngassa, F. N.; Thomasson, K. A.; Gellman, S. H. *Angew. Chem., Int. Ed.* **2004**, *43*, 505. (b) Schmitt, M. A.; Weisblum, B.; Gellman, S. H. *J. Am. Chem. Soc.* **2004**, *126*, 6848. (c) Schmitt, M. A.; Choi, S. H.; Guzei, I. A.; Gellman, S. H. *J. Am. Chem. Soc.* **2005**, *127*, 13130. (d) Sadowsky, J. D.; Schmitt, M. A.; Lee, H.-S.; Umezawa, N.; Wang, S.; Tomita, Y.; Gellman, S. H. *J. Am. Chem. Soc.* **2005**, *127*, 11966. (e) Sadowsky, J. D.; Fairlie, W. D.; Hadley, E. B.; Lee, H. S.; Umezawa, N.; Nikolovska-Coleska, Z.; Wang, S. M.; Huang, D. C. S.; Tomita, Y.; Gellman, S. H. *J. Am. Chem. Soc.* **2007**, *129*, 139. (f) Schmitt, M. A.; Weisblum, B.; Gellman, S. H. *J. Am. Chem. Soc.* **2007**, *129*, 417. (g) Price, J. L.; Horne, W. S.; Gellman, S. H. *J. Am. Chem. Soc.* **2007**, *129*, 6376. (h) Choi, S. H.; Guzei, I. A.; Gellman, S. H. *J. Am. Chem. Soc.* **2007**, *129*, 13780. (i) Choi, S. H.; Guzei, I. A.; Spencer, L. C.; Gellman, S. H. *J. Am. Chem. Soc.* **2008**, *130*, 6544. (j) Schmitt, M. A. Ph. D. Thesis, University of Wisconsin, Madison, 2005.

10.1021/ja808168y CCC: $40.75

or with γ-amino acid residues.[8] Use of α-amino acid residues as one component in a heterogeneous backbone is attractive because the necessary building blocks are commercially available in enantiopure form with a wide diversity of side-chain groups.

Several research groups have explored the folding behavior of short α/β-peptides (≤10 residues) containing a 1:1 α:β backbone pattern.[4−6] Computational work from Hofmann et al., involving a completely unsubstituted α/β-peptide backbone, has identified a number of helical conformations that might be accessible to this type of oligomer.[6a] Four different types of helical secondary structure have been experimentally observed to date; both the substitution pattern on the β-residues and the relative configuration of the α- and β-residues influence the folding preference. Zerbe, Reiser, and co-workers showed that a helix containing i,i−2 C═O···H−N hydrogen bonds is formed when the β-residues have a *cis*-cyclopropyl constraint.[5a] We found that β-residues with a *trans*-cyclopentyl constraint, as in *trans*-2-aminocyclopentanecarboxylic acid (ACPC) residues, promote formation of two types of helix, one with i,i+3 C═O···H−N hydrogen bonds and the other with i,i+4 hydrogen bonds.[4a] (These hydrogen bond connectivities occur as well in the 3_{10}- and α-helix, respectively, which are the most common helical secondary structures observed for the homogeneous α-residue backbone.) Similar folding behavior has been observed by Jagadeesh et al. for α/β-peptides in which the β-residues have a *cis*-disubstituted tetrahydrofuran structure.[5f] Sharma, Kunwar, and co-workers have discovered a helix in which i,i+3 and i,i−1 hydrogen bonds alternate along the backbone, which occurs in heterochiral α/β-peptides containing acyclic β-residues.[5b,c]

We have recently begun to expand beyond 1:1 alternation of α- and β-residues by examining oligomers with 2:1 and 1:2 backbone patterns.[7a] Two-dimensional NMR data obtained for 2:1 heptamer **1** and 1:2 hexamer **2** in methanol revealed numerous NOEs between protons on nonadjacent residues, which provide strong evidence for folding in this relatively polar solvent. We were able to crystallize a nonpolar analogue of 2:1 hepta-α/β-peptide **1** (designated **5** below) and a nonpolar analogue of 1:2 hexa-α/β-peptide **2** (designated **8** below); in both cases the conformation adopted in the solid state contains i,i+3 C═O···H−N hydrogen bonds. However, these conformations could not explain all of the observed NOE patterns for either type of α/β-peptide. Specifically, both the 2:1 and the 1:2 α/β-peptides displayed i,i+3 β-residue C_βH−β-residue C_αH NOEs, but the corresponding H···H distances in the crystal structures were too long to give rise to this type of NOE. These observations can be rationalized by hypothesizing that oligomers **1** and **2** form two different helical conformations in solution, one defined by i,i+3 C═O···H−N hydrogen bonds, as seen in the crystal structures, and one defined by i,i+4 C═O···H−N hydrogen bonds. If, for each α/β-peptide backbone, the two helical conformations interconvert rapidly on the NMR time scale, then one should observe for both **1** and **2** a composite of the NOEs that are characteristic of the two types of helix. This hypothesis was supported by computational models of the 2:1 and 1:2 α/β-peptide backbones in their respective i,i+4 C═O···H−N hydrogen-bonded helix conformations, which suggested that in both cases the i,i+3 β-residue C_βH−β-residue C_αH juxtaposition would be close enough to give rise to an NOE. In addition, this hypothesis is consistent with our previous observations for 1:1 α/β-peptides.[4i] (Terminology note: in past work we have named α/β-peptide helices on the basis of the number of atoms in the characteristic C═O···H−N hydrogen bonds. Thus, for example, the i,i+3 hydrogen-bonded helix of 1:1 α/β-peptides was named the 11-helix. Extending this terminology to 2:1 and 1:2 α/β-peptides becomes cumbersome; the i,i+3 hydrogen bonding pattern gives rise to the 10/11/11-helix and the 11/11/12-helix, respectively. Applying this nomenclature to more complex α/β patterns would be even more unwieldy. We therefore identify helical secondary structures here in terms of the hydrogen bond pattern, that is, i,i+3 or i,i+4 C═O···H−N hydrogen-bonded helix.)

This paper describes trends among 12 α/β-peptide crystal structures, 10 of which are new (Chart 1). The structure set includes five α/β-peptides with the 2:1 backbone pattern (**3**−**7**), ranging in length from 5 to 10 residues, and seven α/β-peptides with a 1:2 backbone pattern (**8**−**14**), which contain from 6 to 11 residues. All of the β-residues in these oligomers are derived from (*S*,*S*)-ACPC. Most of the α-residues are derived from α-aminoisobutyric acid (Aib), because our previous efforts to establish a structural data set for 1:1 α/β-peptides suggested that this subunit is conducive to crystallization;[4i] however, some of the α/β-peptides contain L-alanine or L-phenylalanine. Each of the 12 α/β-peptides displays a fully helical conformation in the solid state, and each helix contains the i,i+3 hydrogen bonding pattern. This data set allows us to establish archetypal structural parameters for the i,i+3 hydrogen-bonded helical

(5) (a) De Pol, S.; Zorn, C.; Klein, C. D.; Zerbe, O.; Reiser, O. *Angew. Chem., Int. Ed.* **2004**, *43*, 511. (b) Sharma, G. V. M.; Nagendar, P.; Jayaprakash, P.; Krishna, P. R.; Ramakrishna, K. V. S.; Kunwar, A. C. *Angew. Chem., Int. Ed.* **2005**, *44*, 5878. (c) Srinivasulu, G.; Kumar, S. K.; Sharma, G. V. M.; Kunwar, A. C. *J. Org. Chem.* **2006**, *71*, 8395. (d) Seebach, D.; Jaun, B.; Sebesta, R.; Mathad, R. I.; Flogel, O.; Limbach, M.; Sellner, H.; Cottens, S. *Helv. Chim. Acta* **2006**, *89*, 1801. (e) Vilaivan, T.; Srisuwannaket, C. *Org. Lett.* **2006**, *8*, 1897. (f) Jagadeesh, B.; Prabhakar, A.; Sarma, G. D.; Chandrasekhar, S.; Chandrashekar, G.; Reddy, M. S.; Jagannadh, B. *Chem. Commun.* **2007**, 371.

(6) (a) Baldauf, C.; Gunther, R.; Hofmann, H. J. *Biopolymers* **2006**, *84*, 408. (b) Zhu, X.; Yethiraj, A.; Cui, Q. *J. Chem. Theory Comput.* **2007**, *3*, 1538. (c) Zhu, X.; Gellman, S. H.; Yethiraj, A.; Cui, Q. *J. Phys. Chem. B* **2008**, *112*, 5439.

(7) (a) Schmitt, M. A.; Choi, S. H.; Guzei, I. A.; Gellman, S. H. *J. Am. Chem. Soc.* **2006**, *128*, 4538. (b) Horne, W. S.; Price, J. L.; Keck, J. L.; Gellman, S. H. *J. Am. Chem. Soc.* **2007**, *129*, 4178. (c) Horne, W. S.; Boersma, M. D.; Windsor, M. A.; Gellman, S. H. *Angew. Chem., Int. Ed.* **2008**, *47*, 2853. (d) Horne, W. S.; Price, J. L.; Gellman, S. H. *Proc. Natl. Acad. Sci. U.S.A.* **2008**, *105*, 9151.

(8) (a) Hagihara, M.; Anthony, N. J.; Stout, T. J.; Clardy, J.; Schreiber, S. L. *J. Am. Chem. Soc.* **1992**, *114*, 6568. (b) Baldauf, C.; Gunther, R.; Hofmann, H. J. *J. Org. Chem.* **2006**, *71*, 1200. (c) Sharma, G. V. M.; Jadhav, V. B.; Ramakrishna, K. V. S.; Narsimulu, K.; Subash, V.; Kunwar, A. C. *J. Am. Chem. Soc.* **2006**, *128*, 14657. (d) Baruah, P. K.; Sreedevi, N. K.; Gonnade, R.; Ravindranathan, S.; Damodaran, K.; Hofmann, H. J.; Sanjayan, G. J. *J. Org. Chem.* **2007**, *72*, 636. (e) Vasudev, P. G.; Ananda, K.; Chatterjee, S.; Aravinda, S.; Shamala, N.; Balaram, P. *J. Am. Chem. Soc.* **2007**, *129*, 4039.

(9) (a) Gong, B.; et al. *Proc. Natl. Acad. Sci. U.S.A.* **2002**, *99*, 11583. (b) Chowdhury, S.; Schatte, G.; Kraatz, H. B. *Angew. Chem., Int. Ed.* **2006**, *45*, 6882. (c) Zhao, Y.; Zhong, Z. Q.; Ryu, E. H. *J. Am. Chem. Soc.* **2007**, *129*, 218. (d) Olsen, C. A.; Bonke, G.; Vedel, L.; Adsersen, A.; Witt, M.; Franzhk, H.; Jaroszewski, J. W. *Org. Lett.* **2007**, *9*, 1549. (e) Angelici, G.; Luppi, G.; Kaptein, B.; Broxterman, Q. B.; Hofmann, H. J.; Tomasini, C. *Eur. J. Org. Chem.* **2007**, 2713. (f) Zhong, Z.; Zhao, Y. *Org. Lett.* **2007**, *9*, 2891. (g) Delsuc, N.; Godde, F.; Kauffmann, B.; Leger, J. M.; Huc, I. *J. Am. Chem. Soc.* **2007**, *129*, 11348.

(10) (a) Cheng, R. P.; Gellman, S. H.; DeGrado, W. F. *Chem. Rev.* **2001**, *101*, 3219. (b) Seebach, D.; Hook, D. F.; Glättli, A. *Biopolymers* **2006**, *84*, 23.

(11) Nelson, J. C.; Saven, J. G.; Moore, J. S.; Wolynes, P. G. *Science* **1997**, *277*, 1793.

(12) (a) Yang, D.; Qu, J.; Bing, L.; Ng, F.-F.; Wang, X.-C.; Cheung, K.-K.; Wang, D.-P.; Wu, Y.-D. *J. Am. Chem. Soc.* **1999**, *121*, 589. (b) Lee, M.-R.; Kim, K.-Y.; Cho, U.-I.; Boo, D. W.; Shin, I. *Chem. Commun.* **2003**, 968.

Chart 1. 2:1 and 1:2 α/β-Peptides (PBB = 4-Bromobenzyl)

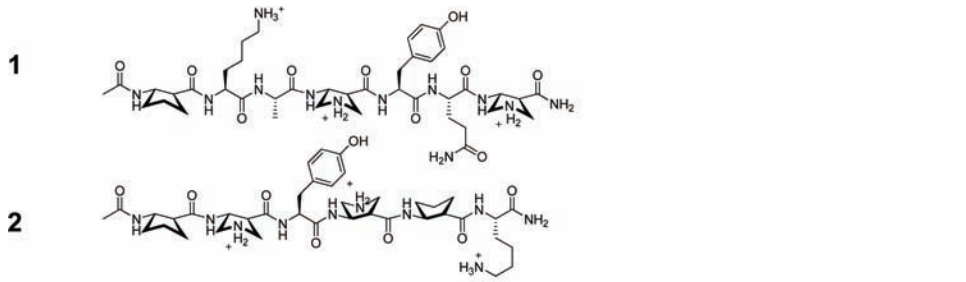

3 Boc-Aib-Aib-ACPC-Aib-Aib-OBn
4 Boc-Aib-Aib-ACPC-Aib-Aib-ACPC-OBn
5 Boc-ACPC-Aib-Aib-ACPC-Aib-Aib-ACPC-OBn

6 Boc-ACPC-(Aib-Ala-ACPC)$_2$-Aib-OPBB
7 Boc-ACPC-(Aib-Ala-ACPC)$_3$-Aib-OPBB

8 Boc-ACPC-ACPC-Phe-ACPC-ACPC-Phe-OBn
9 Boc-ACPC-ACPC-Phe-ACPC-ACPC-Aib-OPBB
10 Boc-ACPC-ACPC-Aib-ACPC-ACPC-Aib-OBn

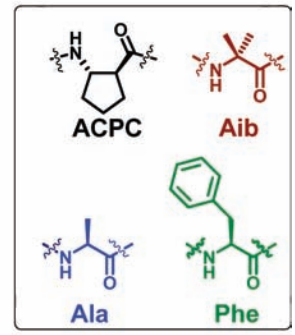

11 Boc-Aib-ACPC-ACPC-Ala-ACPC-ACPC-Aib-OPBB
12 Boc-Ala-ACPC-ACPC-Aib-ACPC-ACPC-Ala-ACPC-ACPC-Aib-OPBB
13 Boc-Aib-ACPC-ACPC-Aib-ACPC-ACPC-Ala-ACPC-ACPC-Aib-OPBB
14 Boc-Aib-ACPC-ACPC-Aib-ACPC-ACPC-Aib-ACPC-ACPC-Aib-OPBB

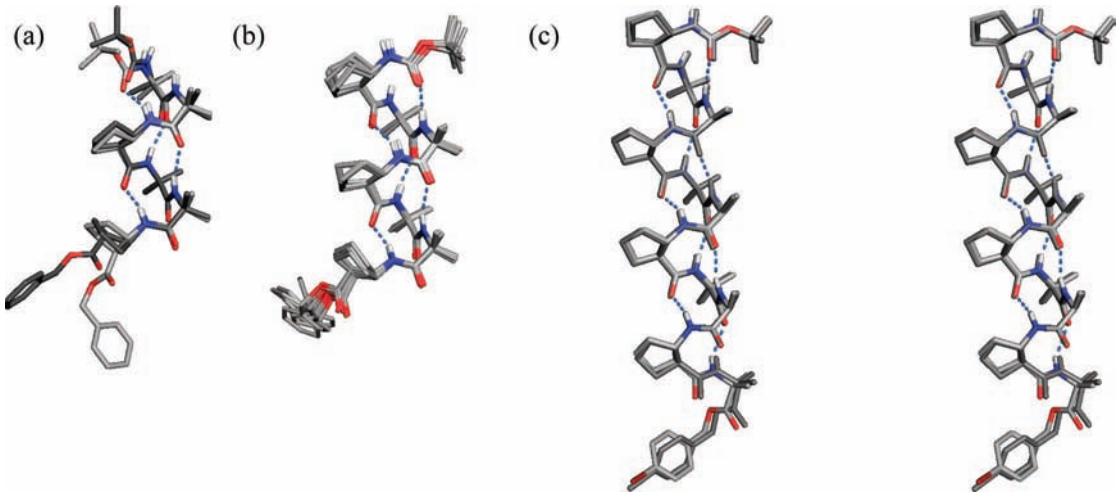

Figure 1. Crystal structures of 2:1 α/β-peptides. All symmetry-independent conformations in the unit cell are overlaid: (a) hexamer **4**, (b) heptamer **5**, and (c) undecamer **7** (stereoview). Dashed lines indicate intramolecular hydrogen bonds. Some hydrogen atoms are omitted for clarity.

secondary structures formed by 2:1 and 1:2 α/β-peptides and to compare these parameters with those of the α-peptide helices (α and 3_{10}), the 1:1 α/β-peptide helices, and the β-peptide helix favored by ACPC residues.

Results and Discussion

Synthesis. Each of the α/β-peptides discussed below was prepared in solution via carbodiimide-mediated coupling reactions, as described previously.[4h,i] Fragment condensation, involving dimeric and trimeric subunits, was used to construct these oligomers. All α/β-peptides have benzylic esters at the C-terminus. Some examples bear a C-terminal *p*-bromobenzyl ester; the heavy atom was incorporated to facilitate crystallographic analysis.

Crystals of most of the α/β-peptides were generated by solvent diffusion of diethyl ether into a chloroform solution of the oligomer. Crystals of **3**, **4**, and **10** were grown by slow evaporation of water−methanol solutions. Crystals of **14** were grown by slow evaporation of a methanol solution.

2:1 α/β-Peptide Structures. Each of the five α/β-peptides with a 2:1 backbone pattern forms the maximum number of *i*,*i*+3 C═O···H−N hydrogen bonds in the solid state, ranging from three for pentamer **3** to nine for undecamer **7**. Three of these five α/β-peptides display multiple independent conformations in the same crystal, but in each case all of the conformations are quite similar. Figure 1a shows an overlay of the two solid-state conformations observed for hexamer **4**. The main differences occur at the C-terminus, which cannot participate in the

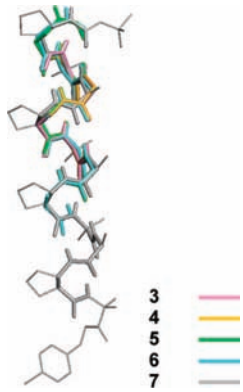

Figure 2. Overlay of five backbone structures of 2:1 α/β-peptides observed in the crystalline state. For **4**, **5**, and **7**, only one independent conformation is shown. The full structure of **7** is drawn with thin lines.

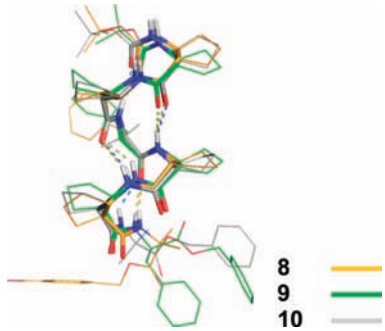

Figure 3. Overlay of three crystal structures of 1:2 α/β-peptide hexamers (**8**−**10**). For **10**, only one conformation is shown. Co-crystallized solvent molecules are omitted for clarity. Backbone atoms (C_α, C_β, C═O, N−H) are highlighted with thick lines. Dashed lines indicate intramolecular hydrogen bonds. Some hydrogen atoms are omitted for clarity.

intramolecular hydrogen bonding pattern because the ester lacks a hydrogen bond donor. Heptamer **5** displays seven distinct conformations in the crystal; these are overlaid in Figure 1b. The differences among the seven conformations are subtle, including variations in cyclopentane ring pucker and in C-terminal benzyl ester position. Figure 1c shows, in stereo, an overlay of the two very similar conformations observed for undecamer **7**. Figure 2 shows a superimposition of conformations observed for **3**−**6** (only one conformation for **4** and **5**) on one of the conformations of **7**. This image illustrates the consistency among the helical conformations adopted by these five α/β-peptides in the solid state.

1:2 α/β-Peptide Structures. Each of the seven α/β-peptides with a 1:2 backbone pattern forms the maximum number of *i*,*i*+3 C═O···H−N hydrogen bonds in the solid state, ranging from four for hexamers **8**−**10** to eight for decamers **12**−**14**. In contrast to the propensity for multiple independent conformations observed among the crystalline 2:1 α/β-peptides, most of the 1:2 α/β-peptides display only a single conformation in the crystalline form (there are two very similar conformations for hexamer **10**). Figure 3 shows an overlay of the solid-state conformations observed for hexamers **8**−**10**. The backbones are very similar, with modest variations in cyclopentane pucker. The largest differences among these structures involve the C-terminal ester groups. Figure 4a shows a stereoview of decamer **14**. Figure 4b provides an overlay for heptamer **11** and all three decamers; the backbones are quite similar except for the termini and variations in cyclopentane pucker. Figure 4c compares views of the three decamers along the helical axis. Differences are apparent from this perspective: **14** has an almost perfect repeat of three residues per turn, but the helical repeats of **12** and **13** deviate somewhat from three residues. These subtle structural variations presumably reflect in some way the tolerance of the 1:2 α/β-peptide *i*,*i*+3 hydrogen-bonded helix to conformational distortion.

The conformational variations among **12**−**14** revealed in Figure 4c may arise from differences in crystal packing, which, in turn, may be related to differences in the solvent molecules that are included in each of these crystals. Decamer **12** co-crystallized with one diethyl ether molecule per α/β-peptide, **13** co-crystallized with three chloroform molecules per α/β-peptide, and **14** co-crystallized with three methanol molecules per α/β-peptide. The locations of these solvent molecules relative to the α/β-peptide are shown in Figure 5. For **12** and **13**, the included solvent molecules pack against the side of the helical α/β-peptide, while for **14** the included solvent molecules cluster around the C-terminus. Thus, solvent molecule packing may cause small distortions of the helical backbones for **12** and **13** relative to **14** in these crystalline forms.

Relationships between H···H Distances and Conformationally Diagnostic NOEs. Table 1 shows the NOE patterns observed previously for **1** and **2** involving protons from residues that are not adjacent in sequence.[4j,7a] For the 2:1 α/β-peptide, four *i*,*i*+2 and three *i*,*i*+3 NOE patterns were observed, and for the 1:2 α/β-peptide, three *i*,*i*+2 and two *i*,*i*+3 NOE patterns were observed. Our crystal structure data set allows us to make multiple independent measurements of the corresponding H···H distances for all but one of these NOE patterns. (The *i*,*i*+2 α-residue C_αH−β-residue NH distances could not be measured for 2:1 α/β-peptides **3**−**7** because every relevant α-residue in these molecules is Aib, which lacks an α-proton.) In addition to H···H distances that correspond to observed NOEs, we find four short H···H distances (<4 Å) in the crystal structures of 1:2 α/β-peptides that do not correspond to NOEs observed in previous NMR studies. These H···H distances are indicated in Table 1. These NOEs could not have been observed in the α/β-peptides we examined by NMR because of resonance overlap. For both α/β-peptide backbones, 2:1 and 1:2, only one of the observed NOE patterns is inconsistent with the *i*,*i*+3 hydrogen-bonded helical conformations seen in the crystals. In both families, the average *i*,*i*+3 β-residue C_βH−β-residue C_αH distance is >5 Å. This finding confirms our previous tentative conclusion, based on molecular modeling, that this particular NOE pattern cannot be explained by the *i*,*i*+3 hydrogen-bonded helical conformations. The modeling led us to propose that this NOE pattern can be explained by *i*,*i*+4 hydrogen-bonded helical conformations. Unfortunately this hypothesis cannot be assessed with the structure set reported here, because the *i*,*i*+4 hydrogen-bonded helix does not occur in any of the crystals. Recently, however, we have observed the *i*,*i*+4 hydrogen-bonded helix for 33-residue oligomers with a 2:1 α:β repeat.[7d] Some or all of the β-residues in these α/β-peptides lack the cyclic constraint (β^3-residues rather than ACPC). In the crystalline forms, these 33-mers self-associate to form tetramers in which each oligomer is helical. The average *i*,*i*+3 β-residue C_βH−β-residue C_αH distance for these *i*,*i*+4 hydrogen-bonded helical structures is <3 Å, which is sufficiently short for NOEs to be observed. To date, there are no crystal structure data for the *i*,*i*+4 hydrogen-bonded helix we have proposed for the 1:2 α/β-peptide backbone.

Backbone Torsion Angle Analysis. The set of 12 structures allows us to identify average backbone torsion angles for the

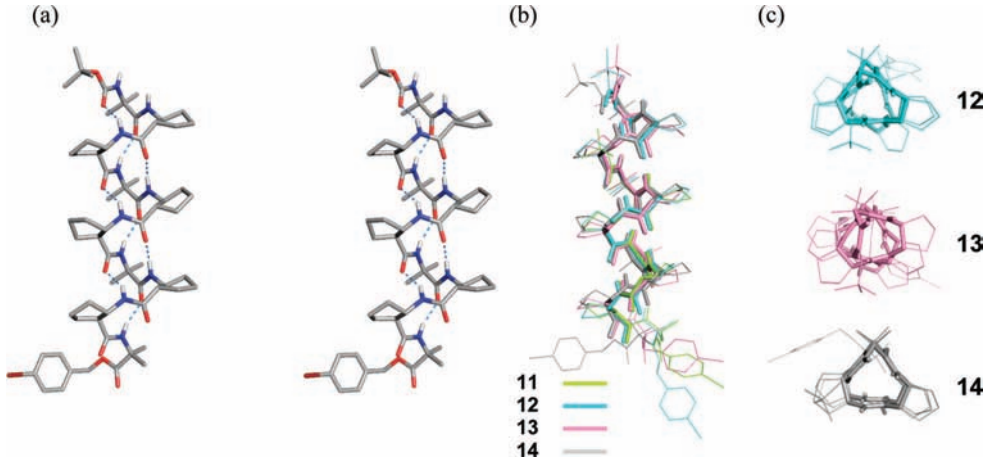

Figure 4. Crystal structures of 1:2 α/β-peptides (**11**−**14**): (a) decamer **14** (stereoview), (b) overlay of four structures, and (c) views of three decamer structures (**12**−**14**) along the helical axis. Backbone atoms (C_α, C_β, C═O, N−H) are highlighted with thick lines. Dashed lines indicate intramolecular hydrogen bonds. Some hydrogen atoms are omitted for clarity.

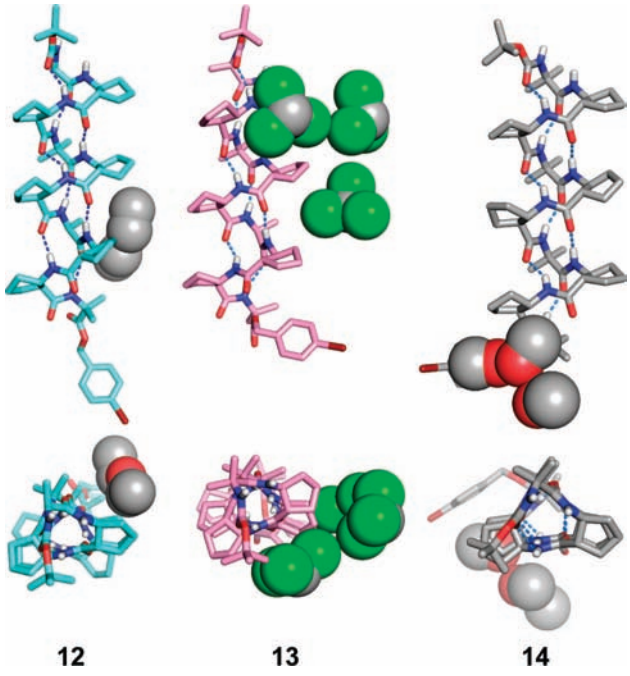

Figure 5. Crystal structures of 1:2 α/β-peptide decamers (**12**−**14**) with co-crystallized solvent molecules: one ether molecule for **12**, three chloroform molecules for **13**, and three methanol molecules for **14**. The upper views are perpendicular to the helical axis, and the lower views are along the helical axis. Solvent molecules are drawn as space-filling models. Dashed lines indicate intramolecular hydrogen bonds. Some disordered atoms for **14** and most hydrogen atoms are omitted for clarity.

i,*i*+3 hydrogen-bonded helices adopted by 2:1 and 1:2 α/β-peptides. The data are presented in Ramachandran-type plots in Figure 6,[13] and the average torsion angles are listed in Table 2. The ϕ and ψ backbone torsion angles for β-residues are defined by analogy to α-residues, and the "extra" backbone torsion angle of β-residues (about the $C_\alpha-C_\beta$ bond) is designated θ, by recent convention.[10a] For both the 2:1 and 2:1 α/β-peptide backbones, the α-residue ψ torsion angles are similar to those observed for a canonical 3_{10}-helix, which shares the *i*,*i*+3 C═O···H−N hydrogen bonding pattern. However, the α-residue ϕ angles in these two α/β-peptide backbones do not match those of the 3_{10}-helix but are instead similar to those of a canonical α-helix (*i*,*i*+4 hydrogen bonds). Previously we found for 1:1 α/β-peptides that the *i*,*i*+3 hydrogen-bonded helix ("11-helix") has an average α-residue ψ torsion angle (−40°) that lies between the values for the 3_{10}- and α-helices, which deviates from the behavior documented here for the 2:1 and 1:2 backbones. The average α-residue ϕ torsion angle (−56°) in the 11-helix is comparable to that found in the α-helix. The three β-residue torsion angles for the helical 2:1 and 1:2 α/β-peptides are similar to the corresponding torsion angles in the 11-helix adopted by 1:1 α/β-peptides.

Helical Parameter Analysis. Average parameters for the *i*,*i*+3 C═O···H−N hydrogen-bonded helices formed by 2:1 and 1:2 α/β-peptides were derived from the structural data as described previously (Table 3). Each helical parameter was calculated from a set of four consecutive α-carbons by a reported method.[14] Nonhelical residues at C-termini were excluded from these calculations. For β-residues, the midpoint between the C_α and C_β atoms was used as an imaginary α-carbon. A total of 17 sets of parameters were derived from the five 2:1 α/β-peptide structures; these parameters were averaged to generate the values in Table 3. Similarly, 28 sets of parameters were derived from the seven 1:2 α/β-peptide structures and averaged. Table 3 includes for comparison helical parameters for three other helices that contain *i*,*i*+3 hydrogen bonds: the α-peptide 3_{10}-helix, the 1:1 α/β-peptide 11-helix, and the β-peptide 12-helix. The parameters for all five helices are quite similar.

Relationships among α/β-Peptide Backbones with Different Backbone Patterns: *i*,*i*+3 vs *i*,*i*+4 Hydrogen-Bonded Helical Propensities. The *i*,*i*+4 C═O···H−N hydrogen-bonded helical conformation was not observed for any of the 2:1 or 1:2 α/β-peptide crystal structures reported here, despite the fact that data for other α/β-peptides suggest that this type of helix is accessible for both backbones. As mentioned above, the medium-range NOE patterns observed for **1** and **2** in methanol cannot be fully explained by *i*,*i*+3 hydrogen-bonded helical conformations; however, these NOE patterns *can* be explained if we propose that both the *i*,*i*+3 and *i*,*i*+4 hydrogen-bonded helices are populated for each type of α/β-peptide, with

(13) Ramachandran, G. N.; Sasisekharan, V. *Adv. Protein Chem.* **1968**, *23*, 283.

(14) (a) Sugeta, H.; Miyazawa, T. *Biopolymers* **1967**, *5*, 673. (b) Kahn, P. C. *Comput. Chem.* **1989**, *13*, 185.

(15) Barlow, D. J.; Thornton, J. M. *J. Mol. Biol.* **1988**, *201*, 601.

Table 1. Average H···H Distances (Å) Corresponding to Medium-Range NOE Patterns

NOE type	distance (Å)[c]	
	i, *i*+3[d]	*i*, *i*+4[d,e]
2:1 α/β-Peptide		
β-residue $C_\beta H(i)$−α-residue NH(*i*+2)[a]	3.3(4) [8]	4.2(3) [9]
β-residue $C_\alpha H(i)$−α-residue NH(*i*+2)[a]	4.3(1) [8]	4.5(1) [9]
α-residue $C_\alpha H(i)$−β-residue NH(*i*+2)	N/A[f]	4.7(3) [10]
α-residue $C_\alpha H(i)$−α-residue NH(*i*+2)	3.6(4) [5]	4.8(1) [11]
β-residue $C_\beta H(i)$−β-residue NH(*i*+3)	3.6(3) [8]	3.2(3) [9]
β-residue $C_\beta H(i)$−β-residue $C_\alpha H(i+3)$	5.9(5) [6]	2.8(2) [10]
α-residue $C_\alpha H(i)$−α-residue NH(*i*+3)	3.6(3) [3]	3.5(4) [18]
β-residue $C_\beta H(i)$−α-residue NH(*i*+2)	3.2(4) [17]	
1:2 α/β-Peptide		
β-residue $C_\beta H(i)$−β-residue NH(*i*+2)	3.4(3) [10]	
β-residue $C_\beta H(i)$−β-residue $C_\alpha H(i+2)$[b]	3.3(4) [10]	
α-residue $C_\alpha H(i)$−β-residue $C_\alpha H(i+2)$[b]	3.2(3) [6]	
α-residue $C_\alpha H(i)$−β-residue NH(*i*+2)[b]	3.8(2) [6]	
β-residue $C_\alpha H(i)$−β-residue NH(*i*+2)	4.1(2) [10]	
β-residue $C_\beta H(i)$−β-residue NH(*i*+3)	3.4(4) [20]	
α-residue $C_\alpha H(i)$−α-residue NH(*i*+3)[b]	3.8(2) [6]	
β-residue $C_\beta H(i)$−β-residue $C_\alpha H(i+3)$	5.3(3) [20]	

[a] NOE types reported for a 2:1 α/β-peptide decamer in ref 4j (see Supporting Information), but not observed for heptamer **1** (ref 7a). Other NOE types listed here for 2:1 α/β-peptide were observed for both the decamer discussed in ref 4j and heptamer **1**. [b] NOEs not observed for **2** (ref 7a) but expected for the 1:2 α/β-peptide on the basis of the average interproton distances from the crystal structures of **8**−**14**. [c] The number in brackets indicates the number of distances measured from the crystal structures. [d] Hydrogen bonding pattern. [e] Average distances derived from the 2:1 α/β-peptide 33-mer (PDB ID 3C3G; resolution, 1.8 Å; estimated coordinate error, 0.15 Å; ref 7d). [f] The distance measurement is not available because the relevant residues have no α-proton.

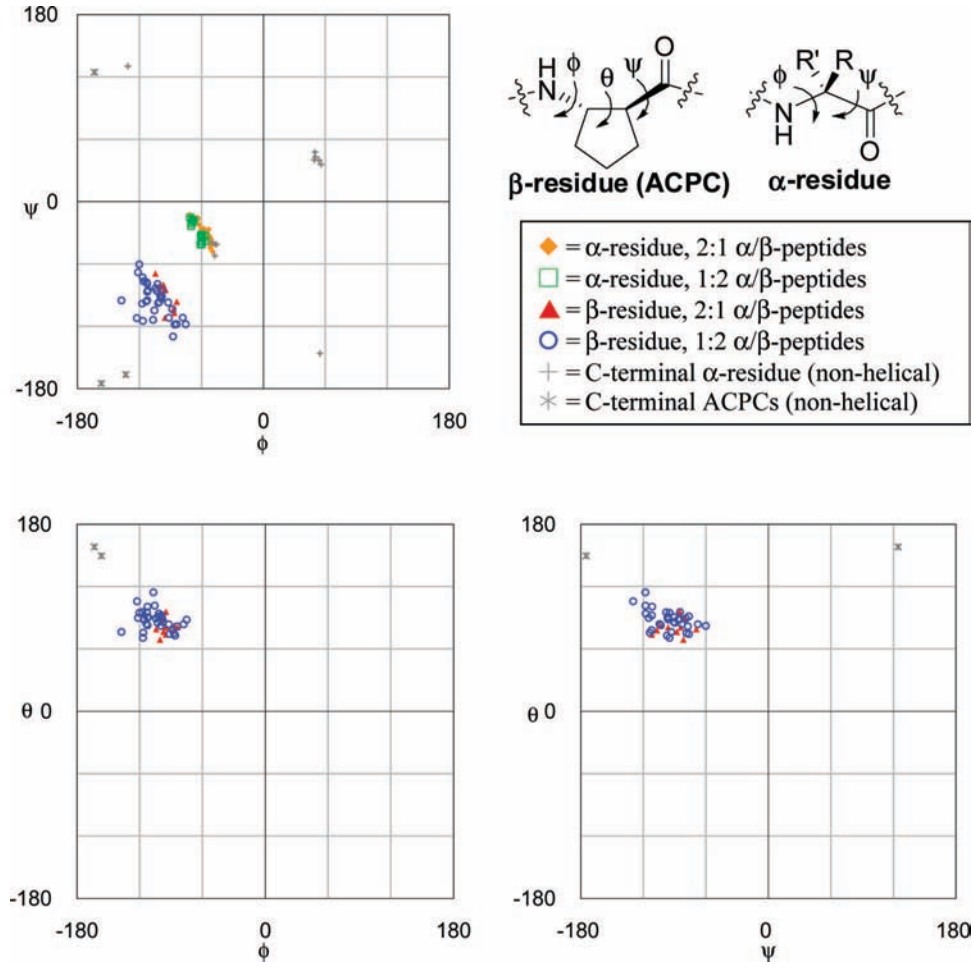

Figure 6. Ramachandran-type plots for the 2:1 and 1:2 α/β-peptide *i*,*i*+3 hydrogen-bonded helices.

rapid interconversion between the helices on the NMR time scale. In addition, the observation of *i*,*i*+4 hydrogen-bonded helical secondary structures for longer crystalline 2:1 α/β-peptides (33 residues) demonstrates that this type of helix is available to this backbone.[7a,d] Indirect evidence is provided by the information available for 1:1 α/β-peptides containing ACPC

Table 2. Average Backbone Torsion Angles (deg) for *i*,*i*+3 Hydrogen-Bonded Helices

	2:1 α/β-peptide[a]		1:2 α/β-peptide[a]		1:1 α/β-peptide[b]		α-peptide[c]
	α-residue	β-residue	α-residue	β-residue	α-residue	β-residue	α-residue
ϕ	−57(7) [21]	−94(6) [11]	−63(5) [14]	−104(14) [24]	−56	−99	−49
ψ	−29(10) [21]	−90(13) [11]	−30(9) [14]	−95(16) [24]	−40	−88	−26
θ		81(8) [11]		88(10) [24]		93	

[a] The number in brackets indicates the number of torsion angles measured from the crystal structures. For **4**, **5**, **7**, and **10**, only one independent conformation was counted. [b] The 11-helix, ref 4i. [c] The 3_{10}-helix, ref 13.

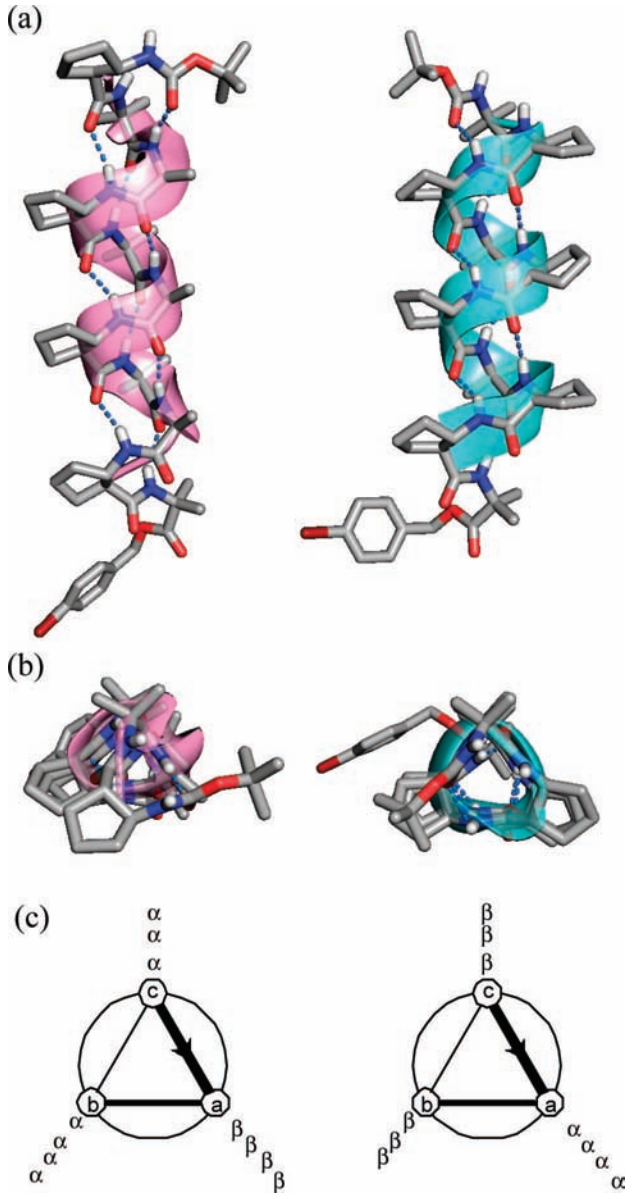

Figure 7. Representation of *i*,*i*+3 hydrogen-bonded helices for 2:1 and 1:2 α/β-peptides and the corresponding helical wheel diagrams: (a) views perpendicular to the helical axis, (b) views along the helical axis, and (c) helical wheel diagrams. Undecamer **7** (on the left) and decamer **14** (on the right) are shown as representative structures for 2:1 and 1:2 α/β-peptides, respectively.

and similarly constrained β-residues, among which both the *i*,*i*+3 and *i*,*i*+4 hydrogen-bonded helical conformations (designated the 11- and 14/15-helices) have been characterized crystallographically. Extensive NOE analysis of 1:1 α/β-peptide oligomers containing six to eight residues yields results comparable to those obtained from 2:1 and 1:2 α/β-peptides: the complete set of NOEs observed for 1:1 α/β-peptides cannot

Table 3. Average Parameters for *i*,*i*+3 Hydrogen-Bonded Helices

peptide backbone (helix type)	res/turn, *n*	rise/turn, *p* (Å)	rise/res, *d* (Å)	radius, *r* (Å)
2:1 α/β-peptide	2.9(1)	5.8(3)	2.0(1)	2.0(1)
1:2 α/β-peptide	2.9(2)	5.5(2)	1.9(1)	2.1(1)
1:1 α/β-peptide (the 11-helix)[a]	2.8	5.6	2.0	2.1
α-peptide (the 3_{10}-helix)[b]	3.2	5.8	1.8	2.0
β-peptide (the 12-helix)[c]	2.6	5.4	2.1	2.3

[a] Reference 4i. [b] Reference 15. [c] References 10a and 16b.

be explained without invoking both helical conformations.[4a] NOE analysis for 15-residue 1:1 α/β-peptides indicates that the *i*,*i*+4 hydrogen-bonded helix becomes dominant with increasing oligomer length (an analogous trend, favoring the α-helix over the 3_{10}-helix, is observed among α-peptides).[4b] This length-dependent trend is manifested among the 14 crystal structures we have obtained for 1:1 α/β-peptides containing ACPC.[4i] Eleven of the structures, for α/β-peptides containing 4−8 residues, show mostly or entirely the *i*,*i*+3 hydrogen bonding pattern, and three of the structures, containing 9 or 10 residues, show exclusively the *i*,*i*+4 hydrogen bonding pattern. In contrast, we observe only *i*,*i*+3 C═O···H−N hydrogen bonds among the longest 2:1 and 1:2 α/β-peptides crystallized, an 11-mer in the 2:1 series and three 10-mers in the 1:2 series.

We propose that the ability of an α/β-peptide to adopt both a helical conformation containing *i*,*i*+3 C═O···H−N hydrogen bonds and a helical conformation containing *i*,*i*+4 C═O···H−N hydrogen bonds depends upon the presence of α-amino acid residues in the foldamer backbone. This hypothesis is based on three considerations. First, pure α-residue backbones can adopt both types of helix (3_{10}-helix and α-helix, respectively). Second, as noted above, 1:1 α/β-peptides have been definitively shown to adopt both types of helix. Third, the *i*,*i*+3 C═O···H−N hydrogen-bonded helix (known as the "12-helix") has been clearly documented among pure β-residue oligomers, if most or all residues contain a five-membered ring constraint;[16] however, the *i*,*i*+4 C═O···H−N hydrogen-bonded helix has not been detected among β-peptides. This last point leads us to

(16) (a) Appella, D. H.; Christianson, L. A.; Klein, D. A.; Powell, D. R.; Huang, X.; Barchi, J. J.; Gellman, S. H. *Nature* **1997**, *387*, 381. (b) Applequist, J.; Bode, K. A.; Appella, D. H.; Christianson, L. A.; Gellman, S. H. *J. Am. Chem. Soc.* **1998**, *120*, 4891. (c) Appella, D. H.; Christianson, L. A.; Klein, D. A.; Richards, M. R.; Powell, D. R.; Gellman, S. H. *J. Am. Chem. Soc.* **1999**, *121*, 7574. (d) Wang, X.; Espinosa, J. F.; Gellman, S. H. *J. Am. Chem. Soc.* **2000**, *122*, 4821. (e) Barchi, J. J.; Huang, X.; Appella, D. H.; Christianson, L. A.; Durell, S. R.; Gellman, S. H. *J. Am. Chem. Soc.* **2000**, *122*, 2711. (f) Lee, H.-S; Syud, F. A.; Wang, X.; Gellman, S. H. *J. Am. Chem. Soc.* **2001**, *123*, 7721. (g) Woll, M. G.; Fisk, J. D.; LePale, P. R.; Gellman, S. H. *J. Am. Chem. Soc.* **2002**, *124*, 12447. (h) LePale, P. R.; Fisk, J. D.; Porter, E. A.; Weisblum, B.; Gellman, S. H. *J. Am. Chem. Soc.* **2002**, *124*, 6820. (i) Park, J.-S.; Lee, H.-S; Lai, J. R.; Kim, B. M.; Gellman, S. H. *J. Am. Chem. Soc.* **2003**, *125*, 8539. (j) Peelen, T. J.; Chi, Y.; English, E. P.; Gellman, S. H. *Org. Lett.* **2004**, *6*, 4411.

speculate that, for α/β-peptides containing ACPC and similarly constrained β-residues, the propensity to form the *i*,*i*+4 C═O···H−N hydrogen-bonded helix will diminish as the α:β ratio becomes smaller. Thus, our failure to observe the *i*,*i*+4 C═O···H−N hydrogen-bonded helix among the 1:2 α/β-peptide crystal structures reported here may reflect a relatively low propensity to adopt this type of helix and the fact that we were not able to crystallize members of this family containing more than 10 residues. The non-appearance of the *i*,*i*+4 hydrogen-bonded helix among our 2:1 α/β-peptide structures is more puzzling. However, only one of our 2:1 α/β-peptides, 11-mer **7**, contains more than eight residues, and in this case the adoption of the *i*,*i*+3 hydrogen-bonded helix in the solid state may reflect the impact of crystal packing forces. It is noteworthy that we have recently determined crystal structures for several 33-residue α/β-peptides with α:β ratios ranging between 2:1 and 3:1, and all display *i*,*i*+4 C═O···H−N hydrogen-bonded helical conformations.[7b,d]

Conclusions

The set of crystal structures reported here provides atomic-resolution structural characterization of two foldameric secondary structures, the *i*,*i*+3 C═O···H−N hydrogen-bonded helices formed by backbones that contain either a 2:1 or a 1:2 repeating pattern of α- and β-amino acid residues. The structural parameters deduced from multiple sets of crystallographic data for each backbone family show that these new folding patterns are comparable to *i*,*i*+3 hydrogen-bonded helices formed by pure α-residue oligomers (the 3_{10}-helix), by pure β-residue oligomers (the 12-helix), and by oligomers containing a 1:1 α:β repeat (the 11-helix). On the basis of these results, it seems likely that similar *i*,*i*+3 hydrogen-bonded helical conformations will be available to backbones with any proportion or pattern of α- and β-residues. Whether or not such helical conformations are significantly populated, however, will depend on factors such as residue substitution patterns, length, and environment.

Experimental Section

General. α-Amino acid derivatives were purchased from Sigma-Aldrich, NovaBiochem, and Chem-Impex International. ACPC-containing dipeptide segments were synthesized by the previously reported procedures.[4i,16c] Reaction time and yield were not optimized. For peptide coupling, EDCI (1.5 equiv)/HOBt (1.3 equiv)/DIEA (1.2 equiv) or EDCI (1.5 equiv)/DMAP (1.1 equiv) were used as coupling reagents. After the coupling reaction was complete, the mixture was diluted with excess EtOAc, and the organic solution was washed with 10% aqueous citric acid, aqueous saturated $NaHCO_3$, and brine. The organic layer was dried over $MgSO_4$, filtered, and concentrated to give a crude product, which was purified by silica gel chromatography.

Boc-Aib-Aib-OBn (15). HCl·H-Aib-OBn was coupled with Boc-Aib-OH to give the desired dipeptide: ^{1}H NMR (300 MHz, $CDCl_3$) δ 7.34 (m, 5H), 5.15 (s, 2H), 1.56 (br s, 6H), 1.43 (br s, 15H); ESI-TOF MS *m/z* calculated for $C_{20}H_{30}N_2O_5$ 378.2, found 379.4 $[M+H]^+$, 401.4 $[M+Na]^+$, 779.7 $[2M+Na]^+$.

Boc-Aib-Aib-ACPC-OEt (16). Boc-Aib-ACPC-OEt[4i] was treated with 4.0 M HCl in dioxane (∼10 equiv). The mixture was stirred for 30 min and then concentrated under a nitrogen gas stream to give the HCl salt form of the amine segment, which was coupled with Boc-Aib-OH to give the desired tripeptide: ^{1}H NMR (300 MHz, $CDCl_3$) δ 7.36 (d, J = 7.7 Hz, 1H), 6.34 (s, 1H), 4.89 (s, 1H), 4.43 (quintet, J = 6.8 Hz, 1H), 4.12 (q, J = 7.1 Hz, 2H), 2.75 (q, J = 7.2 Hz, 1H), 2.13−1.94 (m, 2H), 1.93−1.66 (m, 4H), 1.48 (s, 3H), 1.47 (s, 9H), 1.44 (br s, 6H), 1.42 (s, 3H), 1.23 (t, J = 7.1 Hz, 3H); ESI-TOF MS *m/z* calculated for $C_{21}H_{37}N_3O_6$ 427.3, found 428.5 $[M+H]^+$, 450.5 $[M+Na]^+$, 878.0 $[2M+Na]^+$.

Boc-Aib-Aib-ACPC-Aib-Aib-OBn (3). To a 0.1 M solution of **16** in MeOH/H_2O (v/v = 2/1) at 0 °C was added LiOH·H_2O (5 equiv), and the mixture was stirred for 6 h at 0 °C. After most of the solvent was evaporated by a nitrogen gas stream, aqueous 1 M HCl was added until pH ∼2. The turbid mixture was extracted with EtOAc. The combined organic fraction was washed with brine, dried over $MgSO_4$, filtered, and concentrated in vacuo to give Boc-Aib-Aib-ACPC-OH (**17**), which was used without purification. Dipeptide **15** was treated with 4 M HCl in dioxane to give the HCl salt form of the amine segment, which was coupled with **17** to give pentamer **3**. The X-ray quality crystal was grown by slow evaporation of a methanol/water mixture: ^{1}H NMR (300 MHz, $CDCl_3$) δ 8.07 (s, 1H), 7.69 (d, J = 9.4 Hz, 1H), 7.54 (s, 1H), 7.40−7.22 (m, 5H), 6.91 (s, 1H), 5.13 (s, 2H), 4.26 (m, 1H), 2.36 (q, J = 8.2 Hz, 1H), 2.08−1.90 (m, 2H), 1.87−1.60 (m, 4H), 1.57 (s, 3H), 1.53 (s, 3H), 1.48 (s, 3H), 1.47 (s, 9H), 1.46 (s, 3H), 1.45 (s, 3H), 1.35 (br s, 6H), 1.34 (s, 3H); ESI-TOF MS *m/z* calculated for $C_{34}H_{53}N_5O_8$ 659.4, found 660.8 $[M+H]^+$, 1342.5 $[2M+Na]^+$.

Boc-Aib-Aib-ACPC-OBn (18). To a 0.1 M solution of **17** (1 equiv) in acetonitrile were added benzyl bromide (2 equiv) and K_2CO_3 (3 equiv). The mixture was stirred for 12 h. Tripeptide **18** was isolated from the reaction mixture by the general procedure described above: ^{1}H NMR (300 MHz, $CDCl_3$) δ 7.40 (d, J = 7.8 Hz, 1H),7.36−7.27 (m, 5H), 6.45 (s, 1H), 5.13 (ABq, J_{AB} = 12.6 Hz, $\Delta\upsilon$ = 0.06 ppm, 2H), 5.03 (s, 1H), 4.49 (quintet, J = 7.2 Hz, 1H), 2.83 (m, 1H), 2.14−1.98 (m, 2H), 1.91−1.55 (m, 4H), 1.45 (s, 3H), 1.44 (s, 9H), 1.41 (s, 3H), 1.40 (s, 3H), 1.39 (s, 3H); ESI-TOF MS *m/z* calculated for $C_{26}H_{39}N_3O_6$ 489.3, found 490.5 $[M+H]^+$, 512.4 $[M+Na]^+$, 1001.9 $[2M+Na]^+$.

Boc-Aib-Aib-ACPC-Aib-Aib-ACPC-OBn (4). Compound **4** was prepared from **17** and **18**: ^{1}H NMR (300 MHz, $CDCl_3$) δ 7.82 (s, 1H), 7.68 (d, J = 7.5 Hz), 7.60 (d, J = 9.5 Hz), 7.53 (s, 1H), 7.43−7.27 (m, 5H), 6.56 (s, 1H), 5.15 (ABq, J_{AB} = 12.6 Hz, $\Delta\upsilon$ = 0.08 ppm, 2H), 5.13 (s, 1H), 4.53 (m, 1H), 4.23 (m, 1H), 3.09 (dt, J = 8.8, 4.6 Hz, 1H), 2.33 (q, J = 8.3 Hz, 1H), 2.22−1.60 (m, 12H), 1.67 (s, 3H), 1.58 (s, 3H), 1.52 (s, 3H), 1.50 (s, 3H), 1.47 (s, 9H), 1.45 (s, 3H), 1.40 (s, 3H), 1.39 (s, 3H), 1.36 (s, 3H); ESI-TOF MS *m/z* calculated for $C_{40}H_{62}N_6O_9$ 770.5, found 771.9 $[M+H]^+$, 793.9 $[M+Na]^+$.

Other 2:1 and 1:2 α/β-peptides were prepared by a fragment condensation strategy analogous to that described above. Further experimental details can be found in the Supporting Information.

Acknowledgment. This work was supported by NSF grant CHE-0551920. S.H.C. was supported in part by a fellowship from the Samsung Scholarship Foundation. We thank Dr. W. Seth Horne for helpful comments. X-ray equipment purchase was supported in part by grants from the NSF.

Supporting Information Available: Complete ref 9a, characterization data, crystallographic information, and full table of helical parameters (PDF, CIF). This material is available free of charge via the Internet at http://pubs.acs.org.

JA808168Y